MOLECULAR AND CELLULAR BIOLOGY, Aug. 2007, p. 5381–5392 Vol. 27, No. 15
0270-7306/07/$08.00+0 doi:10.1128/MCB.00282-07

Hypoxia-Inducible Factor Linked to Differential Kidney Cancer Risk Seen with Type 2A and Type 2B *VHL* Mutations▽†

Lianjie Li,[1,2] Liang Zhang,[3] Xiaoping Zhang,[3] Qin Yan,[1,2] Yoji Andrew Minamishima,[1] Aria F. Olumi,[3] Mao Mao,[4] Steven Bartz,[4] and William G. Kaelin, Jr.[1,2]*

Department of Medical Oncology, Dana-Farber Cancer Institute and Brigham and Women's Hospital, Harvard Medical School, Boston, Massachusetts 02115[1]; Howard Hughes Medical Institute, Chevy Chase, Maryland 20815[2]; Department of Urology, Beth Israel Deaconess Medical Center, Harvard Medical School, Boston, Massachusetts 02115[3]; and Rosetta Inpharmatics LLC, Seattle, Washington 98109[4]

Received 15 February 2007/Returned for modification 1 April 2007/Accepted 17 May 2007

Clear cell carcinoma of the kidney is a major cause of mortality in patients with von Hippel-Lindau (VHL) disease, which is caused by germ line mutations that inactivate the *VHL* tumor suppressor gene. Biallelic *VHL* inactivation, due to mutations or hypermethylation, is also common in sporadic clear cell renal carcinomas. The *VHL* gene product, pVHL, is part of a ubiquitin ligase complex that targets the alpha subunits of the heterodimeric transcription factor hypoxia-inducible factor (HIF) for destruction under well-oxygenated conditions. All *VHL* mutations linked to classical VHL disease compromise this pVHL function although some missense mutations result in a low risk of kidney cancer (type 2A VHL disease) while others result in a high risk (type 2B VHL disease). We found that type 2A mutants were less defective than type 2B mutants when reintroduced into $VHL^{-/-}$ renal carcinoma cells with respect to HIF regulation. A stabilized version of HIF2α promoted tumor growth by $VHL^{-/-}$ cells engineered to produce type 2A mutants, while knock-down of HIF2α in cells producing type 2B mutants had the opposite effect. Therefore, quantitative differences with respect to HIF deregulation are sufficient to account for the differential risks of kidney cancer linked to *VHL* mutations.

von Hippel-Lindau (VHL) disease is an autosomal dominant hereditary cancer syndrome caused by germ line mutations of the *VHL* tumor suppressor gene and is characterized by an increased risk of tumor development in multiple organs, such as hemangioblastoma of the central nervous system, pheochromocytoma of the adrenal glands, and clear cell carcinoma of the kidneys (36). Tumor development occurs when the remaining wild-type allele is inactivated. Kidney cancer develops in ~75% of VHL patients by age 60 and is a leading cause of death in this population (70). In keeping with the Knudson two-hit model, somatic *VHL* mutations leading to *VHL* inactivation are also common in sporadic clear cell renal cell carcinomas (RCC) and restoration of *VHL* function in $VHL^{-/-}$ RCC is sufficient to suppress tumor formation in vivo (21, 30).

The *VHL* gene product, pVHL, is the substrate recognition component of an E3 ubiquitin ligase complex that also contains elongin B, elongin C, Cul2, and Rbx1 (15, 16, 33, 39–42, 52, 64). pVHL has two functional domains, the α domain and the β domain, which are involved in the direct binding to elongin C and pVHL substrates, respectively (42, 45, 52, 62, 76). The α domain is also important for pVHL stability since pVHL mutants defective in elongin C binding are unstable and rapidly degraded (71). The best characterized pVHL target is the alpha subunit of hypoxia-inducible factor (HIF). HIF is a heterodimeric transcription factor consisting of an oxygen-sensitive α subunit and a stable β subunit. In the presence of oxygen, one (or both) of two conserved prolyl residues in the oxygen-dependent degradation domain of HIFα is hydroxylated by members of the EglN family of iron-dependent dioxygenases (5, 17, 27, 31, 32, 34, 56, 58, 77). Prolyl-hydroxylated HIFα is recognized by pVHL, polyubiquitinated, and thereby targeted for proteasomal degradation (35, 37). Accordingly, wild-type cells express low levels of HIFα in the presence of oxygen but accumulate high levels of HIFα under low-oxygen conditions (57). Cells lacking pVHL contain high levels of HIFα regardless of oxygen tension.

HIF is a master regulator of the transcriptional activation of hypoxia-inducible genes involved in angiogenesis, glucose uptake, erythropoiesis, cell proliferation, and apoptosis (24, 35, 37, 72). A number of these target genes are implicated in renal carcinogenesis including *TGFA* (transforming growth factor alpha), *PDGF* (platelet-derived growth factor), *VEGF* (vascular endothelial growth factor), *CXCL12* (*SDF-1*α), and *CXCR4* (18, 36, 49, 75, 78). Emerging evidence suggests that HIF2α, among the three mammalian HIFα family members (HIF1α, HIF2α, and HIF3α), is the critical oncogenic pVHL substrate in renal carcinogenesis. First, $VHL^{-/-}$ RCC cell lines express either high levels of both HIF1α and HIF2α or exclusively HIF2α (54, 57). Second, stabilization of HIF2α, but not HIF1α, overcomes the tumor suppressor function of pVHL (48, 55). Third, eliminating HIF2α is sufficient to suppress $VHL^{-/-}$ tumor growth in vivo (47, 79). Finally, overexpression of HIF2α promotes tumor growth, whereas overexpression of HIF1α delays tumor development (69).

* Corresponding author. Mailing address: Dana-Farber Cancer Institute, 44 Binney Street, Mayer 457, Boston, MA 02115. Phone: (617) 632-3975. Fax: (617) 632-4760. E-mail: William_kaelin@dfci.harvard.edu.

† Supplemental material for this article may be found at http://mcb.asm.org/.

▽ Published ahead of print on 25 May 2007.

VHL disease is clinically divided into two types based on the presence (type 2) or the absence (type 1) of pheochromocytoma. Type 2 disease is further subdivided into three subtypes: type 2A (low risk of RCC), type 2B (high risk of RCC), and type 2C (pheochromocytoma only). VHL disease shows clear genotype-phenotype correlations (36, 43). Type 1 disease is associated with large deletions or protein-truncating mutations that grossly compromise pVHL's functions, including its ability to regulate HIFα. In contrast, type 2 disease is almost always linked to *VHL* missense mutations. Interestingly, both type 2A and type 2B *VHL* mutations measurably compromise pVHL's ability to regulate HIF (7, 61, 62, 68). Therefore, it is still not fully understood why type 2A and type 2B *VHL* mutations are associated with markedly different risks of developing renal carcinoma. In this regard, a number of HIF-independent functions have been ascribed to pVHL, some of which might conceivably be linked to renal tumorigenesis (10, 36). On the other hand, a recent report suggested that type 2A mutants bind to HIFα with higher affinity than do type 2B mutants, at least in vitro, raising the possibility that quantitative differences between type 2A and type 2B mutants with respect to HIF binding translate into different risks of renal carcinoma in humans (46).

In the present study, we introduced selected type 2A and type 2B pVHL mutants into a *VHL*$^{-/-}$ RCC cell line and characterized them for their ability to regulate HIFα as well as their ability to suppress RCC tumor growth in nude mice. We found that type 2A and 2B pVHL mutants differ quantitatively with respect to the regulation of HIF2α and HIF target genes, with type 2A being less compromised than type 2B mutants. Furthermore, the increased levels of HIF2α and its downstream targets in cells producing type 2B mutants correlated with increased tumor formation in subcutaneous and orthotopic xenograft assays in nude mice. A causal role for HIF in these assays was supported by experiments in which HIF2α levels were artificially increased in type 2A cells or decreased in type 2 B cells, leading to increased or decreased tumorigenesis, respectively. Our results further strengthen the notion that HIF2α is a critical component in renal carcinogenesis in the setting of *VHL* inactivation.

MATERIALS AND METHODS

Plasmids. pBabe-puro-HA-VHL (where HA is hemagglutinin) was described previously (60). To make pBabe-puro-HA-VHL carrying residues 1 to 115 of VHL [pBabe-puro-HA-VHL(1–115)], pRc-CMV-HA-VHL (where CMV is cytomegalovirus) (30) was PCR amplified with the primers 5′-CGACTCACTAT AGGGAGACCC-3′ and 5′-TTCAGAATTCTCAGTGACCTCGGTAGCTGT GG-3′, digested with BamHI and EcoRI, and ligated into pBabe-Puro-HA (48) cut with these two enzymes. To make pBabe-puro-HA-VHL(Y98H) and pBabe-puro-HA-VHL(L118V), the BamHI-EcoRI fragments from pRc-CMV-HA-VHL with the mutation Y98H (61) and pRc-CMV-HA-VHL with the mutation L188V (62), respectively, were ligated into pBabe-Puro-HA cut with these two enzymes. The pBabe-puro-HA-VHL expression plasmids for all other the pVHL mutants used in this paper were generated by site-directed mutagenesis using pBabe-puro-HA-VHL as the template (primer sequences are available upon request) and confirmed by DNA sequencing.

pBabe-Hygro-HIF2α P405A/P531A (HIF2α dPA) was made by ligating the BamHI-MfeI fragment of pcDNA3.0-HA-HIF2α P405A/P531A (48) into pBabe-Hygro cut with BamHI and EcoRI.

Expression plasmids for short hairpin RNAs (shRNAs) targeting HIF2α were constructed by inserting the EcoRI-HindIII fragments from pRS-2 and pRS-9 (47) into pSUPER-retro-GFP/Neo (OligoEngine) to create shHIF2α(#2) and shHIF2α(#3), respectively. Oligonucleotides for shRNAs targeting luciferase (5′-GATCCCCCGTACGCGGAATACTTCGATTCAAGAGATCGAAGTAT TCCGCGTACGTTTTTA-3′ and 5′-AGCTTAAAAACGTACGCGGAATAC TTCGATCTCTTGAATCGAAGTATTCCGCGTACGGGG-3′) were annealed and ligated into pSUPER-retro-GFP/Neo using unique HindIII and BglII sites within its polylinker.

pGL3-3×HRE-Luc (3×HRE-Luc) (a kind gift from Andrew Kung, Dana-Farber Cancer Institute) was created by inserting three copies of the canonical hypoxia-response element (HRE) and a minimal thymidine kinase promoter into pGL3-Basic (Promega).

Cell culture. 786-O cells (obtained from ATCC) and Phoenix cells (a generous gift from Gary Nolan, Department of Molecular Pharmacology, Stanford University) were maintained in Dulbecco's modified Eagle's medium (DMEM) containing 10% fetal bovine serum or fetal clone I, respectively. 786-O cells stably infected with retroviruses were selected and maintained in the presence of 2 μg/ml puromycin (for pBabe-puro retroviruses) or 0.5 mg/ml hygromycin (for pBabe-Hygro retroviruses). 786-O cells stably infected with shRNA retroviruses were selected in the presence of 1.5 mg/ml of neomycin and subsequently maintained in the presence of 1 mg/ml of neomycin.

Hypoxia treatment was carried out in a hypoxic chamber containing 1% oxygen (Laboratory Products, Inc).

Retroviruses. Retrovial plasmids were transfected into the Phoenix packaging cell line using Lipofectamine 2000 (Invitrogen) according to the manufacturer's instructions. Tissue culture medium was collected 48 h after transfection, passed through a 0.45-μm-pore-size filter, and added to cells in the presence of 8 μg/ml polybrene.

Immunoblotting analysis. Cells were lysed in EBC buffer (50 mM Tris [pH 8.0], 120 mM NaCl, 0.5% NP-40) supplemented with complete protease inhibitor cocktail (Roche Molecular Biochemicals). Protein concentration was determined by the Bradford method (Bio-Rad). Lysates were resolved by sodium dodecyl sulfate-polyacrylamide gel electrophoresis and transferred to nitrocellulose membranes (Bio-Rad). After membranes were blocked in Tris-buffered saline with 5% nonfat dry milk, they were probed with the following primary antibodies: anti-HA mouse monoclonal antibody (HA-11; Covance Research Product), anti-HIF1α rabbit polyclonal antibody (A & G Pharmaceutical), anti-HIF2α mouse monoclonal antibody (NB100-122; Novus Biologicals), anti-Glut1 rabbit polyclonal antibody (GT111-A; Alpha Diagnostic), anti-EglN3 mouse monoclonal antibody (a generous gift from Peter Ratcliffe) (2), antitubulin mouse monoclonal antibody (B-512; Sigma), anti-cyclin D1 rabbit polyclonal antibody (Ab-3; Lab Vision), or anti-cyclin A rabbit polyclonal antibody (C-19; Santa Cruz). Bound antibody was detected with horseradish peroxidase-conjugated goat anti-rabbit or goat anti-mouse antibody (Pierce) and SuperSignal West Pico or Dura chemiluminescent substrate (Pierce).

Microarray experiments. Total RNA was isolated using an RNeasy Mini Kit with on-column DNase digestion (QIAGEN). The method for processing total RNA for hybridization to microarrays containing approximately 25,000 oligonucleotides has been previously described in detail (29). Ratio hybridizations were generated by performing a fluorescent label reversal of the RNA to eliminate dye bias. RNA from cells expressing mutated pVHL was hybridized against RNA from cells expressing wild-type pVHL or empty vector controls. The microarrays used in the experiments were purchased from Agilent Technologies. The error models for data processing have been previously described (29). Data were analyzed using Rosetta Resolver, version 6.0, software.

We clustered experiments by a rank order and clustered a subset of ~270 consensus pVHL-regulated genes (significantly regulated [*P* value of 0.01] in two of three experiments comparing cells infected with retrovirus encoding wild-type pVHL with cells infected with empty vector) using an agglomerative method. We then compared the regulation of these genes by pVHL with the mutation Y98H or Y112H [yielding pVHL(Y98H) or pVHL(Y112H), respectively] relative to wild-type pVHL to their regulation by the corresponding asparagine mutants. A Wilcoxon signed-rank test was used to determine the significance of the differences between histidine and asparagine mutants in their regulation of this cluster of genes.

Luciferase reporter assays. Cells grown in 12-well tissue culture plates were transfected with 0.4 μg of 3×HRE-Luc and 4 ng of pRL-CMV-*Renilla* (Promega) using Lipofectamine 2000 (Invitrogen) according to the manufacturer's instructions. Six hours later cells were incubated under normoxic or hypoxic conditions for 18 h, and luciferase values were measured with a Dual Luciferase Assay System (Promega) according to the manufacturer's instructions using a luminometer (Berthold Technologies). Firefly luciferase values were normalized to *Renilla* luciferase.

In vitro proliferation assays. In vitro cell proliferation assays were performed using a Cell Proliferation Kit II (XTT) (Roche Diagnostics) according to the manufacturer's instructions. Briefly, approximately 1,000 cells were seeded per

well in 96-well plates and grown under the cell culture conditions described above. At the indicated time points, XTT labeling reagent/electron coupling reagent was added to the cells. Four hours later the spectrophotometrical absorbance at 450 nm was measured using a microtiter plate reader (Perkin Elmer Life and Analytical Science).

Three-dimensional multicellular spheroid culture. Multicellular spheroids were prepared as previously described (51). Briefly, 10^5 cells were seeded per well in 24-well tissue culture plates that were precoated with 250 μl of 1% SeaPlaque agarose (Cambrex Bio Science Rockland, Inc.) in DMEM. The plates were gently swirled 30 times before they were returned to the tissue incubator. Half of the medium was replaced with fresh medium after 3 to 4 days. Pictures of spheroids were taken using a phase-contrast microscope (×100 magnification) after 7 days of growth.

Fluorescence-activated cell sorter analysis. Cells were plated at low density (2×10^5 cells per 15-cm plate) and incubated overnight. Cells were either grown for another 48 h before bromodeoxyuridine (BrdU) labeling or were washed with phosphate-buffered saline and incubated in DMEM supplemented with 1% insulin-transferin-selenium (Gibco) for 72 h. The cells were incubated with 10 μM BrdU (Sigma) for 2 h, trypsinized, washed, and fixed in 75% ethanol. Fixed cells were then stained with a fluorescein isothiocyanate- or a phycoerythrin-conjugated anti-BrdU antibody (BD Bioscience) according to the manufacturer's instructions. Stained cells were suspended in phosphate-buffered saline containing 5 μg/ml of propidium iodide (for samples stained with fluorescein isothiocyanate-conjugated anti-BrdU; Roche), or 0.25 μg/ml of 7-aminoactinomycin D for samples stained with phycoerythrin-conjugated anti-BrdU; BD Bioscience). Cells were analyzed on a fluorescence-activated cell sorter (FACScan; Becton Dickinson) using CellQuest software.

Nude mouse xenograft assays. Subcutaneous nude mice xenograft assays were performed as previously described (30). Briefly, 10^7 viable cells, as determined by trypan blue staining, were injected subcutaneously into the flanks of nude mice. The mice were sacrificed 7 to 8 weeks postinjection, and tumors were excised and weighed. Results are presented as mean ± standard error of the mean. Results were evaluated statistically using a two-sided Mann-Whitney Wilcoxon test.

Orthotopic xenograft was performed essentially as described previously (1, 20, 59). Mice were anesthetized with ketamine hydrochloride and xylazine (Xyla-Ject). A 1-cm incision was made along the right flank of the mouse. After the right kidney was exposed, 2×10^6 viable cells were injected near the lower pole into the renal parenchyma. Wounds were closed with absorbable suture, and subsequent renal tumors were monitored by palpation. The mice were sacrificed 9 to 11 weeks after injection as specified in figure legends. Tumor mass was calculated by subtracting the mass of the left kidney (normal) from the mass of the right kidney (implanted with tumor). If the tumor xenograft mass was small and the left kidney was slightly heavier than the right, the mass of the tumor was recorded as zero. The presence or absence of tumors was confirmed histologically after hematoxylin and eosin staining. Results are presented as mean ± standard error of the mean. Results were evaluated statistically using a *t* test.

RESULTS

Type 2A and 2B pVHL mutants differentially regulate HIFα. We infected 786-O and RCC4 *VHL*$^{-/-}$ human renal carcinoma cells with retroviral vectors encoding selected type 2A and type 2B pVHL mutants in an effort to understand the differential risk of RCC linked to type 2A and type 2B germ line *VHL* mutations. As controls, cells were infected with a vector encoding wild-type pVHL (VHL), an empty retrovirus (vector), or a retrovirus encoding a truncated, presumably null, pVHL mutant encompassing residues 1 to 115 [pVHL(1–115)]. For some experiments we also infected 786-O cells to produce pVHL(L188V), which is a canonical type 2C pVHL mutant (7, 25, 26). Type 2C mutants are associated with an increased risk of pheochromocytoma but a low risk of RCC and a low risk of hemangioblastomas. All the mutants were tagged at their N termini with an influenza HA epitope, and the retroviruses contained a puromycin resistance cassette. Successfully infected cells were selected in puromycin-containing medium and maintained as polyclonal pools.

786-O cells produce exclusive HIF2α whereas RCC4 cells produce both HIF1α and HIF2α (57). As expected, HIFα protein levels were suppressed by wild-type pVHL but not by pVHL(1-115) under normoxic conditions (Fig. 1A and B). pVHL(1-115) lacks an intact alpha and beta domain and also accumulated to much lower levels than did wild-type pVHL, probably because it is unstable (71). Notably, type 2A pVHL mutants also suppressed the levels of HIFα and the HIF-responsive gene products Glut1 and cyclin D1, nearly as well as wild-type pVHL (Fig. 1A to C; see also Fig. S1 in the supplemental material). The pVHL levels achieved by retroviral infection were ~10-fold higher than the levels of endogenous pVHL observed in a variety of human cell lines (data not shown), and it is therefore possible that the type 2A defect with respect to HIF regulation would be more pronounced at physiological pVHL concentrations. Nonetheless, type 2A and type 2B mutants demonstrably differed in these assays because HIFα and its targets were clearly elevated in cells producing type 2B mutants, despite their overproduction, relative to wild-type pVHL controls.

These results suggested that type 2A and type 2B mutants differ quantitatively with respect to HIFα regulation. To explore this further, 786-O cells producing different pVHL mutants were transfected with a firefly luciferase reporter plasmid containing three HREs upstream of a minimal thymidine kinase promoter along with a *Renilla* luciferase control plasmid. Firefly luciferase values, normalized to *Renilla* luciferase, were determined 18 h later after growth in 1% (hypoxia) or 21% (normoxia) oxygen (Fig. 1D). As expected, normalized luciferase values were suppressed by wild-type pVHL and pVHL (L188V), especially under normoxic conditions, compared to cells infected with an empty retrovirus or the virus encoding pVHL(1-115). In keeping with the immunoblotting data, type 2A mutants more effectively suppressed HIF-dependent transcription than did type 2B mutants.

Type 2B pVHL mutants, unlike type 2A mutants, fail to promote cell cycle exit by *VHL*$^{-/-}$ renal carcinoma cells upon serum withdrawal. Restoration of wild-type pVHL function in *VHL*$^{-/-}$ human renal carcinoma cells does not affect proliferation in serum-rich medium but does promote cell cycle exit under low-serum conditions and promotes differentiation in spheroid growth assays (12, 14, 22, 51, 63, 74). In keeping with the former, none of the mutants tested here affected 786-O cell proliferation under standard culture conditions (Fig. 2A). Under low-serum conditions, however, cells producing type 2B pVHL mutants were more defective than cells producing type 2A pVHL mutants with respect to their ability to exit the cell cycle, with type 2A cells more closely resembling cells producing wild-type pVHL (Fig. 2B). Failure of type 2B cells to exit the cell cycle correlated with increased levels of cyclin D1 and cyclin A (Fig. 2C). Likewise, cyclin D1 levels in RCC4 cells grown under low-serum conditions were higher in cells producing type 2B mutants than in cells producing type 2A mutants (see Fig. S2 in the supplemental material).

Type 2A and type 2B pVHL mutants differ in spheroid growth assays. *VHL*$^{-/-}$ RCC cells form compact, featureless, spheroids when grown under conditions that foster three-dimensional growth. In contrast, *VHL*$^{-/-}$ RCC cells ectopically producing wild-type pVHL form looser aggregates when

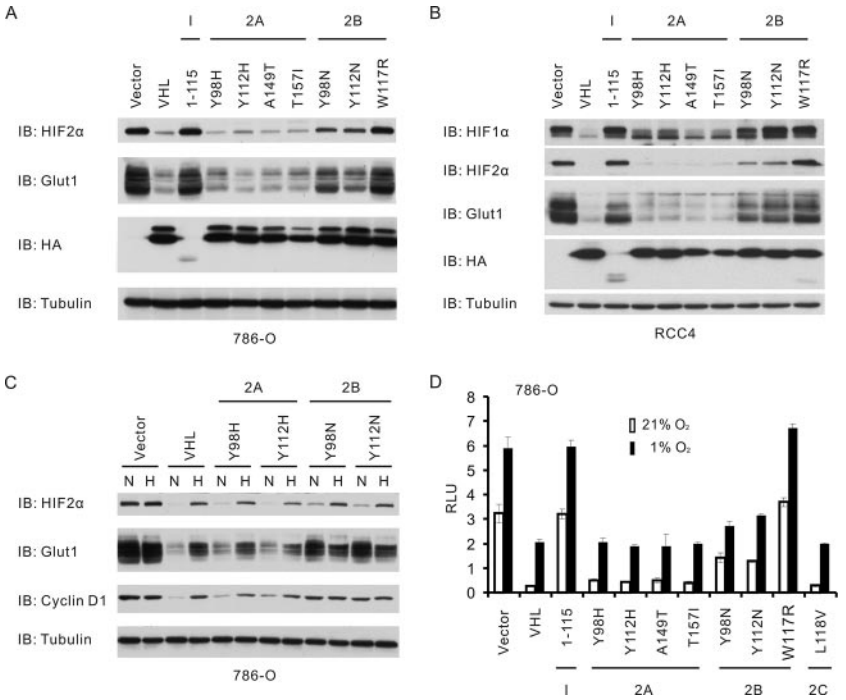

FIG. 1. Differential regulation of HIFα and HIF target genes by type 2A and type 2B pVHL mutants. (A to C) Immunoblot analysis of 786-O (A and C) and RCC4 (B) renal carcinoma cells infected with retroviruses encoding the indicated HA-tagged pVHL variants or with the empty vector. For panel C cells were grown under hypoxic (H; 1% oxygen) or normoxic (N; 21% oxygen) conditions. (D) Firefly luciferase values, normalized to *Renilla* luciferase values, for 786-O cells infected with retroviruses encoding the indicated VHL proteins or with empty vector. Cells were transiently transfected with an HIF-responsive firefly luciferase reporter plasmid and a *Renilla* luciferase control plasmid and grown in the presence of 21% or 1% O_2 for 24 h prior to analysis. RLU, relative light units; IB, immunoblot.

grown under such conditions and assume epithelial characteristics (51). We repeated these assays with cells producing type 2A or type 2B pVHL mutants (Fig. 2D; see also Fig. S3 in the supplemental material). The spheroids producing the type 2A pVHL mutants more closely resembled the spheroids formed by cells infected to produce wild-type pVHL than did the spheroids formed by cells producing type 2B pVHL mutants. Therefore, type 2A and type 2B mutants differ in two in vitro assays of pVHL functions that probably contribute to pVHL's ability to suppress tumor growth in vivo (51, 63).

Global gene expression profiles of type 2A and 2B pVHL mutants reveal quantitative differences. Replacement of pVHL residues Y98 or Y112 with histidine creates a type 2A mutant while replacement of Y98 or Y112 with asparagine creates a type 2B mutant (25). We reasoned that paired mutants affecting the same pVHL residue should be particularly informative with respect to understanding the differential risk of renal carcinoma linked to type 2A and type 2B *VHL* mutations. Toward this end, mRNA was harvested from 786-O cells infected with an empty retrovirus or the retroviruses encoding wild-type pVHL, pVHL(Y98H), pVHL(Y98N), pVHL(Y112H), or pVHL(Y112N) and subjected to microarray analysis. The genes regulated by pVHL(Y98H) were highly similar to those regulated by pVHL(Y98N) and therefore fall along the diagonal in Fig. 3A. pVHL(Y98H), as expected, more closely resembled wild-type pVHL than did pVHL(Y98N) (Fig. 3B). In particular, a subset of HIF target gene mRNAs, such as *EGLN3*, *VEGF*, and *SLC2A1* (*GLUT1*) mRNAs, were increased in cells producing pVHL(Y98N) relative to cells producing pVHL(Y98H) (Fig. 3A, B, and E). Similar results were obtained when pVHL(Y112H) was compared to pVHL(Y112N) (Fig. 3C to E). The increased expression of pVHL target genes in cells producing pVHL (Y98N) or pVHL(Y112N) (relative to cells producing wild-type pVHL) was significantly greater ($P < 10^{-17}$ and $P < 10^{-8}$, respectively) than observed in cells producing the corresponding histidine mutants. These results strengthen the contention that type 2A pVHL mutants are less defective with respect to the regulation of HIF and HIF-responsive genes than type 2B pVHL mutants.

Type 2A pVHL mutants suppress renal carcinoma growth in vivo more effectively than do type 2B pVHL mutants. Next, 786-O cells producing either pVHL(Y98H) or pVHL(Y98N) were injected subcutaneously into the opposite flanks of nude mice to determine their ability to form tumors in vivo. Eight weeks later the animals were sacrificed, and the resulting tumors were excised and weighed. Similar experiments were conducted with cells producing pVHL(Y112H) or pVHL(Y112N). Although biological assays of this type are subject to variation, cells producing the type 2B mutants formed tumors that were significantly larger ($P < 0.05$) than their type 2A counterparts (Fig. 4A and B). Therefore, the differential risk of renal carcinoma linked to these mutations in humans is reflected, at least qualitatively, in nude mouse xenograft assays.

The differences observed in the nude mouse assays between type 2A and type 2B mutants, although statistically significant, were not as striking as the different risks of renal carcinoma

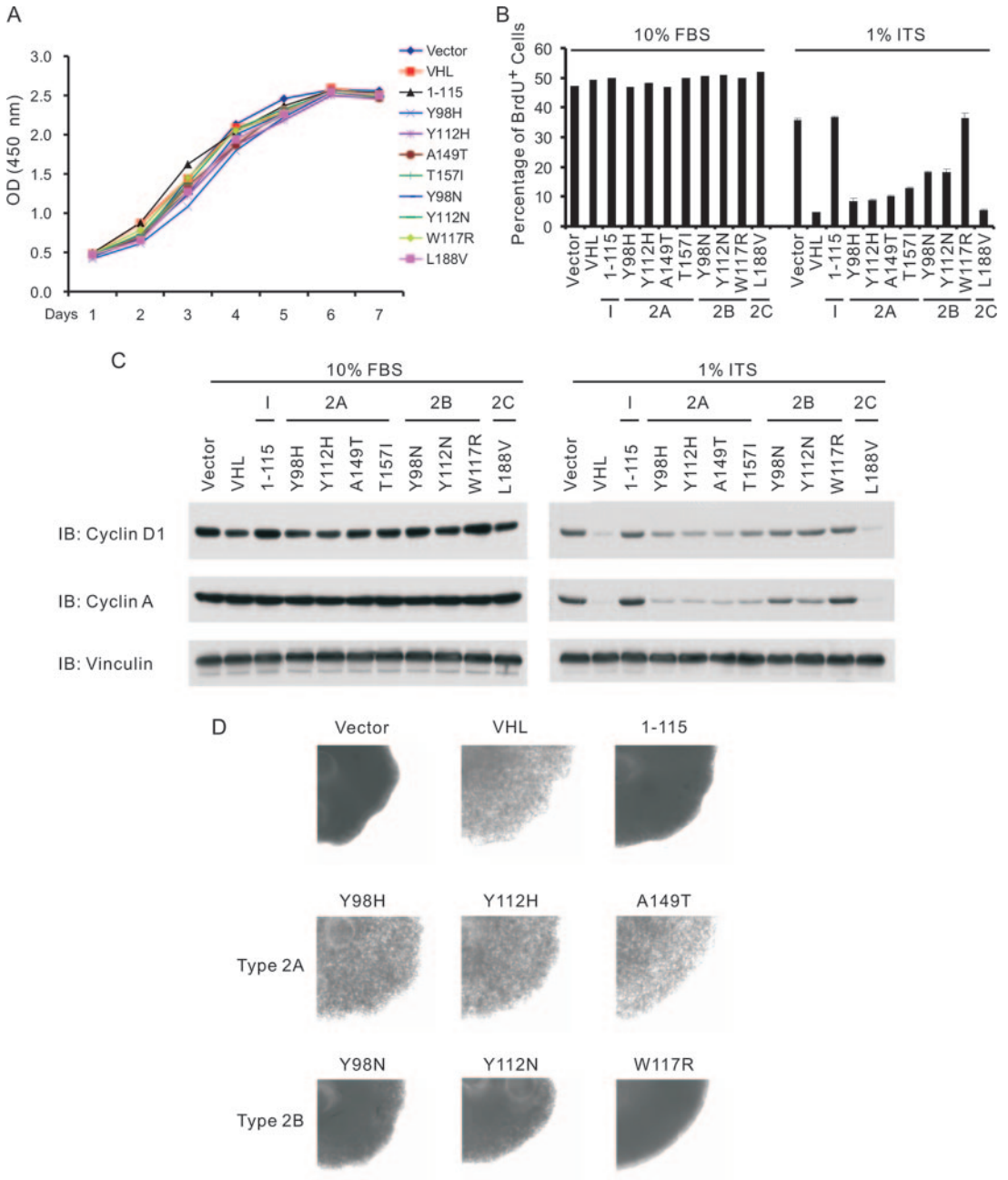

FIG. 2. Proliferation of 786-O cells expressing type 2A or type 2B pVHL mutants in vitro. (A) Optical density (OD) at 450 nm, which reflects viable cell number, of 786-O cells stably infected with retroviruses encoding the indicated pVHL variants and maintained in 10% fetal bovine serum. Standard deviation is <0.2 for all data points. (B and C) BrdU incorporation and immunoblot (IB) analysis of 786-O cells stably infected with retroviruses encoding the indicated pVHL variants and maintained in DMEM containing 10% fetal bovine serum (10% FBS) or in DMEM supplemented with 1% insulin-transferrin-selenium (1% ITS) for 72 h prior to BrdU pulse for 2 h. Error bars in panel B indicate the standard deviations. (D) Multicellular spheroids formed by 786-O cells stably infected with retroviruses encoding the indicated pVHL variants. Spheroids were photographed (magnification, ×100) after 7 days of growth. Note that cells producing type 2B mutants form dense cell spheroids similar to those formed by the vector control cells or the cells expressing pVHL(1–115), a type I mutant. Cells producing wild-type pVHL or type 2A mutants form loose spheroids.

observed in humans bearing these mutations. This might, among several possibilities, reflect the fact that the subcutaneous space in nude mouse does not recapitulate the microenvironment in which pVHL-defective renal carcinoma cells arise in humans. In an attempt to more faithfully model human renal carcinogenesis, 786-O cells producing the different Y98 and Y112 mutants were grown orthotopically in the kidneys of nude mice. Tumors were examined at necropsy approximately 11 weeks later. Y98N- and Y112N-producing cells formed large tumors that were approximately fourfold larger, by mass, than the tumors formed by cells producing the corresponding type 2A mutants (Fig. 4C and D). It therefore appears that the

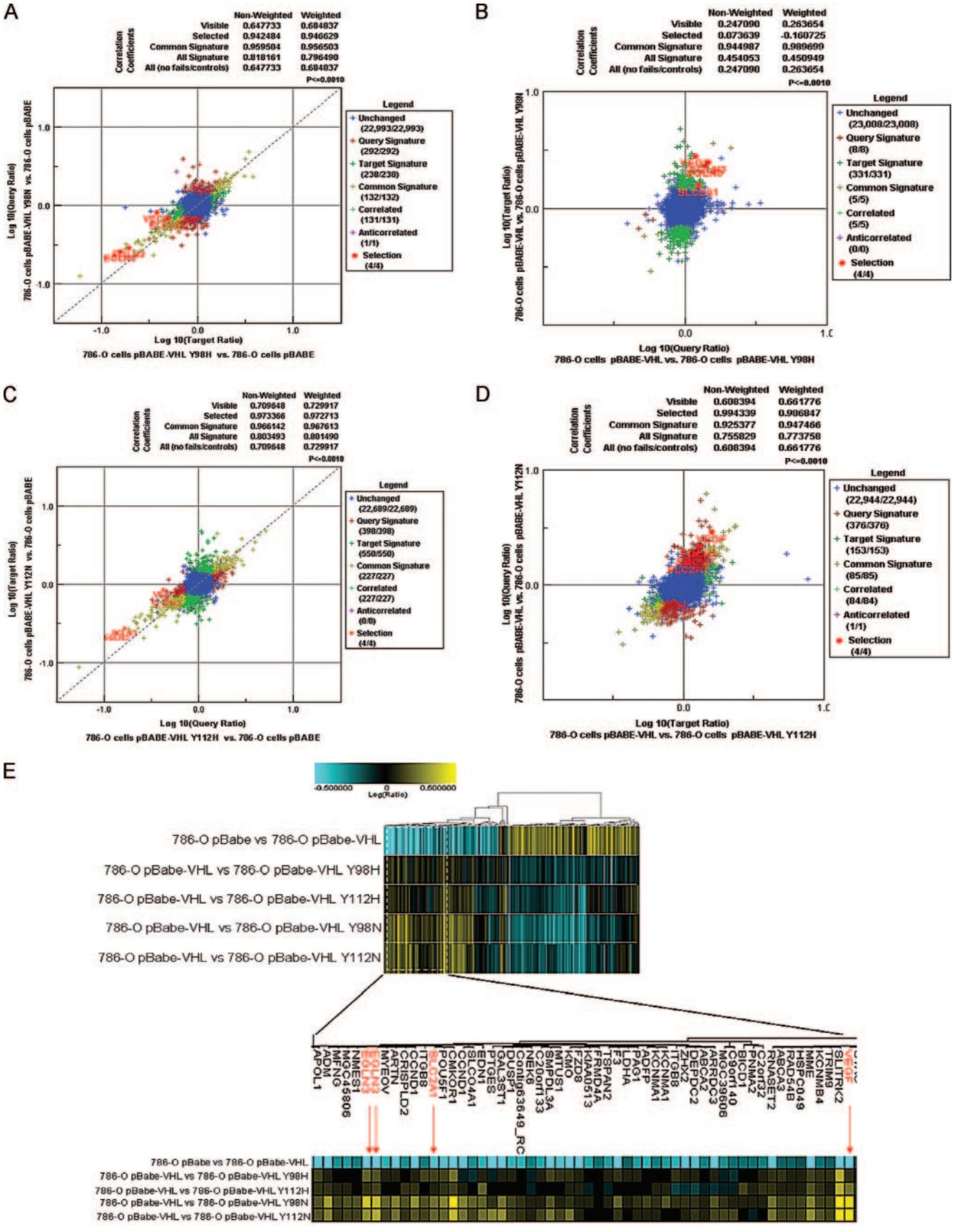
A
Correlation Coefficients
Non-Weighted Weighted
Visible 0.647733 0.684837
Selected 0.942484 0.946629
Common Signature 0.959504 0.956503
All Signature 0.818161 0.796490
All (no fails/controls) 0.647733 0.684837
P<=0.0010
Legend
Unchanged (22,993/22,993)
Query Signature (292/292)
Target Signature (238/238)
Common Signature (132/132)
Correlated (131/131)
Anticorrelated (1/1)
Selection (4/4)
Log 10(Query Ratio)
786-O cells pBABE-VHL Y98N vs. 786-O cells pBABE
Log 10(Target Ratio)
786-O cells pBABE-VHL Y98H vs. 786-O cells pBABE
B
Correlation Coefficients
Non-Weighted Weighted
Visible 0.247090 0.263654
Selected 0.073639 -0.160725
Common Signature 0.944987 0.989699
All Signature 0.454053 0.450949
All (no fails/controls) 0.247090 0.263654
P<=0.0010
Legend
Unchanged (23,008/23,008)
Query Signature (8/8)
Target Signature (331/331)
Common Signature (5/5)
Correlated (5/5)
Anticorrelated (0/0)
Selection (4/4)
Log 10(Target Ratio)
786-O cells pBABE-VHL vs. 786-O cells pBABE-VHL Y98N
Log 10(Query Ratio)
786-O cells pBABE-VHL vs. 786-O cells pBABE-VHL Y98H
C
Correlation Coefficients
Non-Weighted Weighted
Visible 0.709648 0.729917
Selected 0.973366 0.972713
Common Signature 0.966142 0.967613
All Signature 0.803493 0.801490
All (no fails/controls) 0.709648 0.729917
P<=0.0010
Legend
Unchanged (22,689/22,689)
Query Signature (398/398)
Target Signature (550/550)
Common Signature (227/227)
Correlated (227/227)
Anticorrelated (0/0)
Selection (4/4)
Log 10(Target Ratio)
786-O cells pBABE-VHL Y112N vs. 786-O cells pBABE
Log 10(Query Ratio)
786-O cells pBABE-VHL Y112H vs. 786-O cells pBABE
D
Correlation Coefficients
Non-Weighted Weighted
Visible 0.600394 0.661776
Selected 0.994339 0.986847
Common Signature 0.925377 0.947466
All Signature 0.755829 0.773758
All (no fails/controls) 0.608394 0.661776
P<=0.0010
Legend
Unchanged (22,944/22,944)
Query Signature (376/376)
Target Signature (153/153)
Common Signature (85/85)
Correlated (84/84)
Anticorrelated (1/1)
Selection (4/4)
Log 10(Query Ratio)
786-O cells pBABE-VHL vs. 786-O cells pBABE-VHL Y112N
Log 10(Target Ratio)
786-O cells pBABE-VHL vs. 786-O cells pBABE-VHL Y112H
E
-0.500000
0
0.500000
Log(Ratio)
786-O pBabe vs 786-O pBabe-VHL
786-O pBabe-VHL vs 786-O pBabe-VHL Y98H
786-O pBabe-VHL vs 786-O pBabe-VHL Y112H
786-O pBabe-VHL vs 786-O pBabe-VHL Y98N
786-O pBabe-VHL vs 786-O pBabe-VHL Y112N
APOL1
ADM
MFNG
MGC45805
NMES1
ARTN
MYEOV
CRISPLD2
CCND1
ITGB8
CCND1
POU5F1
CMKOR1
SLCO4A1
EDN1
PTGES
GAL3ST1
DUSP3
63649_RC
CENB
C20orf133
SMPDL3A
MTUS1
KMO
FZD8
KIAA0513
FRMD4A
TSPAN2
F3
LDHA
PAG1
ADFP
KCNMA1
KCNMA1
ITGB8
ZHX2
DEPDC2
ABCA2
ARRDC3
MGC39606
C9orf140
BICD1
PNMA2
C2orf32
RNASET2
ABCA3
RAD54B
MSRC049
MMNMB4
TRIM9
SLITRK2
786-O pBabe vs 786-O pBabe-VHL
786-O pBabe-VHL vs 786-O pBabe-VHL Y98H
786-O pBabe-VHL vs 786-O pBabe-VHL Y112H
786-O pBabe-VHL vs 786-O pBabe-VHL Y98N
786-O pBabe-VHL vs 786-O pBabe-VHL Y112N

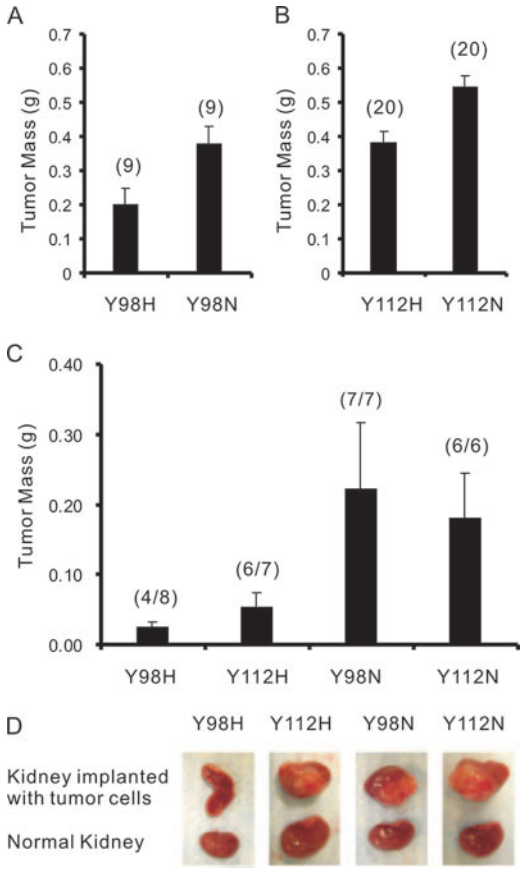

FIG. 4. Type 2B pVHL mutants display higher tumorigenic potential in nude mice than type 2A mutants. (A and B) Masses of tumors formed by 786-O cells stably infected with retroviruses encoding the indicated pVHL variants 8 weeks after subcutaneous injection in nude mice. Each mouse was injected with cells producing a type 2A mutant or the corresponding type 2B mutant on opposite flanks. The number of tumors analyzed is indicated in parentheses. Error bars are 1 standard error of the mean ($P < 0.05$). (C) Calculated masses of tumors formed by 786-O cells stably infected with retroviruses encoding the indicated pVHL variants 11 weeks after intraparenchymal renal injection in nude mice. The presence of tumor cells was confirmed by hematoxylin and eosin staining. The tumor mass was calculated by subtracting the mass of the left kidney (normal) from the mass of the right kidney (implanted with tumor). Numbers in parentheses indicate the number of animals with tumors divided by number of animals injected. Error bars are 1 standard error of the mean ($P < 0.05$). (D) Representative photographs of injected and control kidneys from panel C.

orthotopic model is a more powerful model for discriminating between pVHL mutants associated with different risks of renal cancer in humans.

Differences in HIF2α levels observed in cells producing type 2A versus type 2B pVHL mutants play a causal role in tumorigenesis. We previously showed that inhibition of HIF2α is both necessary and sufficient for pVHL-mediated suppression of renal carcinoma growth in nude mouse assays (47, 48). Therefore, it is likely that the observed differences between the type 2A and type 2B mutants with respect to HIF regulation are responsible for the differences we observed in the nude mouse assays. Nonetheless, one could still argue that HIF is a marker for the relative structural integrity of the type 2A and type 2B mutants and that an HIF-independent pVHL function contributes to the differential risk of renal carcinoma ascribed to type 2A and type 2B mutants. To begin to address this we experimentally manipulated HIF2α levels in cells producing the Y98 and Y112 pVHL mutants.

First, we infected 786-O cells producing pVHL Y98H or Y112H with a retrovirus encoding a HIF2α variant lacking both prolyl hydroxylation sites (HIF2α dPA, lacking Pro405 and Pro531). This mutant escapes recognition by pVHL but retains the ability to activate HIF target genes (47, 48). As expected, HIF2α levels in the infected cells now exceeded those observed in cells producing Y98N or Y112N and led to increased accumulation of HIF-responsive gene products such as cyclin D1 and EglN3 (Fig. 5A) (3, 13, 65, 69). HIF2α dPA did not affect cell proliferation under serum-rich conditions in vitro (Fig. 5B) but did interfere with cell cycle exit upon serum starvation, such that the type 2A cells producing HIF2α dPA more closely resembled cells producing the corresponding type 2B pVHL mutant (Fig. 5C). Likewise, type 2A cells producing HIF2α dPA now more closely resembled type 2B cells with respect to their ability to form tumors in subcutaneous (Fig. 5D and E) and orthotopic (Fig. 5F and G) xenograft assays in nude mouse.

In a reciprocal set of experiments, HIF2α levels were decreased in 786-O cells producing pVHL(Y98N) or pVHL (Y112N) using shRNA technology (47). Infection of cells with either of two retroviruses encoding different shRNAs targeting HIF2α [shHIF2α(#2)and shHIF2α(#3)], but not a control virus targeting luciferase, led to decreased HIF2α levels and decreased expression of the canonical HIF target EglN3 (Fig. 6A). Downregulation of HIF2α did not affect cell growth under serum-rich conditions (Fig. 6B). In contrast, downregulation of HIF2α promoted the cell cycle exit upon serum with-

FIG. 3. Type 2B mutants have decreased ability to regulate VHL-regulated genes relative to type 2A mutants. (A and B) Comparison of genes regulated by Y98N versus empty vector (*y* axis) to genes regulated by Y98H versus empty vector (*x* axis) in 786-O cells (A). Y98N and Y98H have similar effects (hence, most genes lie along diagonal). However, some genes (examples in red font) are repressed more effectively by Y98H than Y98N (therefore, above the diagonal in the lower-left quadrant). This is easier to see in panel B, where Y98H and Y98N are compared to wild-type pVHL to accentuate differences between these two mutants. Genes represented by green plus signs are deregulated in Y98N much more than in Y98H cells. Data shown are representative of two independent experiments. (C and D) Analysis of genes regulated by pVHL(Y112H) or pVHL (Y112N) as in panels A and B. (E) One-dimensional clustering of 786-O cells expressing wild-type pVHL compared to 786-O empty vector cells (top row) or compared to cells producing VHL2A (Y98H and Y112H) or VHL2B (Y98N and Y112N) mutants (bottom four rows) using Rosetta Resolver software. A gene set of consensus pVHL-regulated genes (approximately 270 genes) was used to perform the analysis. The gene set was compiled by requiring a gene to be significantly regulated (*P* value of <0.01) in two of three experiments comparing 786-O cells expressing wild-type pVHL to empty vector cells. In the upper rows of both panels, genes repressed by pVHL are in blue. These genes are more upregulated (yellow) in cells producing 2B mutants than in cells producing 2A mutants when 2A and 2B mutants are compared to wild-type pVHL.

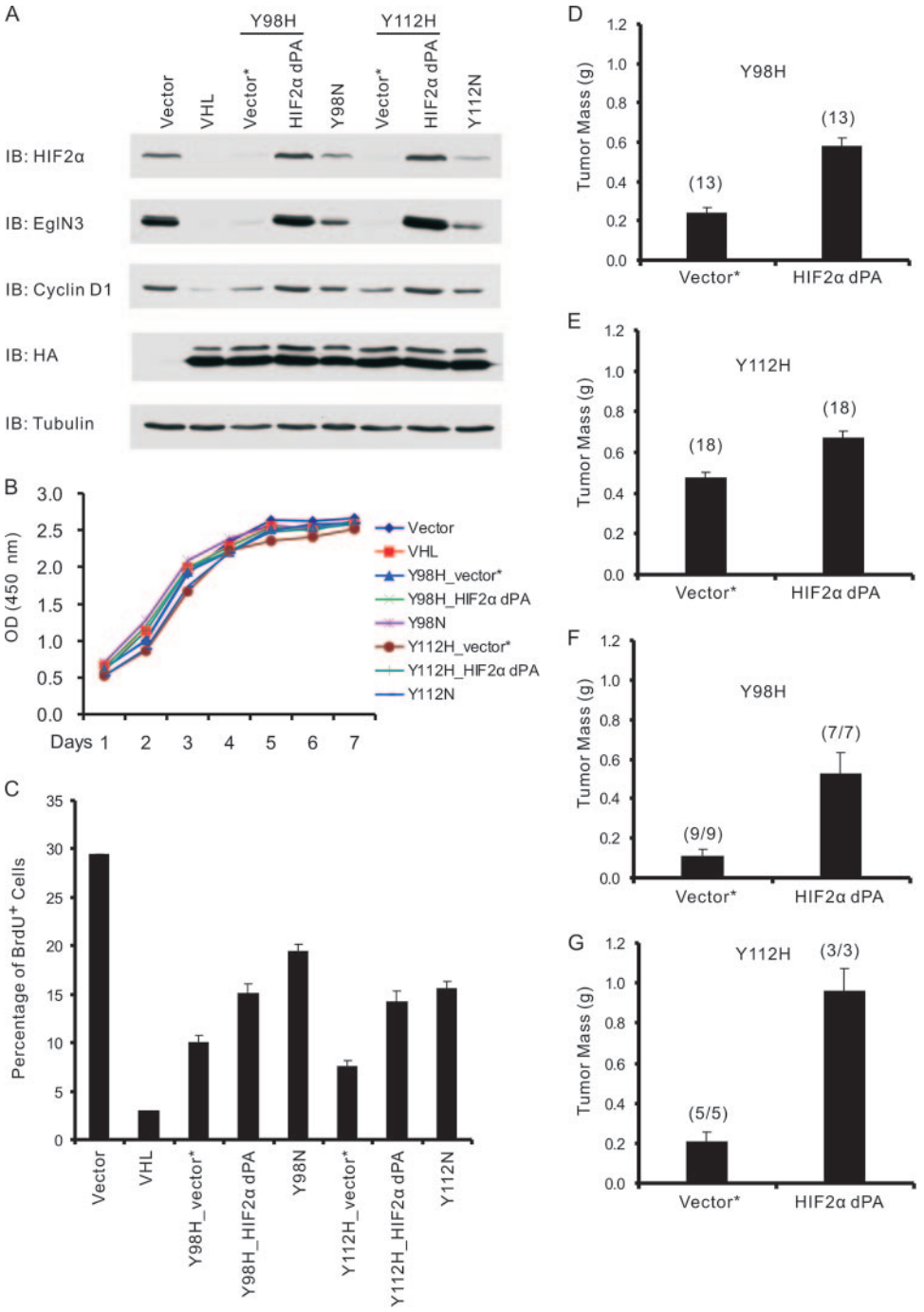

FIG. 5. Stabilizing HIF2α promotes tumor growth by 786-O cells producing type 2A pVHL mutants in vivo. (A) Immunoblot (IB) analysis of 786-O renal carcinoma cells infected with retroviruses encoding the indicated HA-tagged pVHL proteins or with the empty vector (Vector). Where indicated, cells were also infected with a second virus encoding HIF2α dPA (P405A/P531A) or with the corresponding empty virus (Vector*). (B) Optical density (OD) at 450 nm, which reflects viable cell number, of 786-O cells studied in panel A and maintained in 10% fetal bovine serum. The standard deviation is <0.2 for all data points. (C) BrdU incorporation of 786-O cells stably infected with retroviruses as in panel A and maintained in serum-free DMEM supplemented with 1% insulin-transferrin-selenium (1% ITS) for 72 h prior to BrdU pulse for 2 h. Error bars indicate standard deviations. (D and E) Masses of tumors formed by 786-O cells stably infected with retroviruses as in panel A 8 weeks after subcutaneous injection in nude mice. Each mouse was injected with the corresponding empty virus (Vector*) or HIF2α dPA cells on opposite flanks. The number of tumors analyzed is indicated in parentheses. Error bars are 1 standard error of the mean ($P < 0.05$). (F and G) Calculated masses of tumors formed by 786-O cells stably infected with retroviruses as in panel A 10 weeks (Y98H) or 9 weeks (Y112H) after intraparenchymal renal injection in nude mice. The presence of tumor cells was confirmed by hematoxylin and eosin staining. The tumor mass was calculated by subtracting the mass of the left kidney (normal) from the mass of the right kidney (implanted with tumor). Numbers in parentheses indicate the number of animals with tumors divided by number of animals injected. Error bars are 1 standard error of the mean ($P < 0.05$).

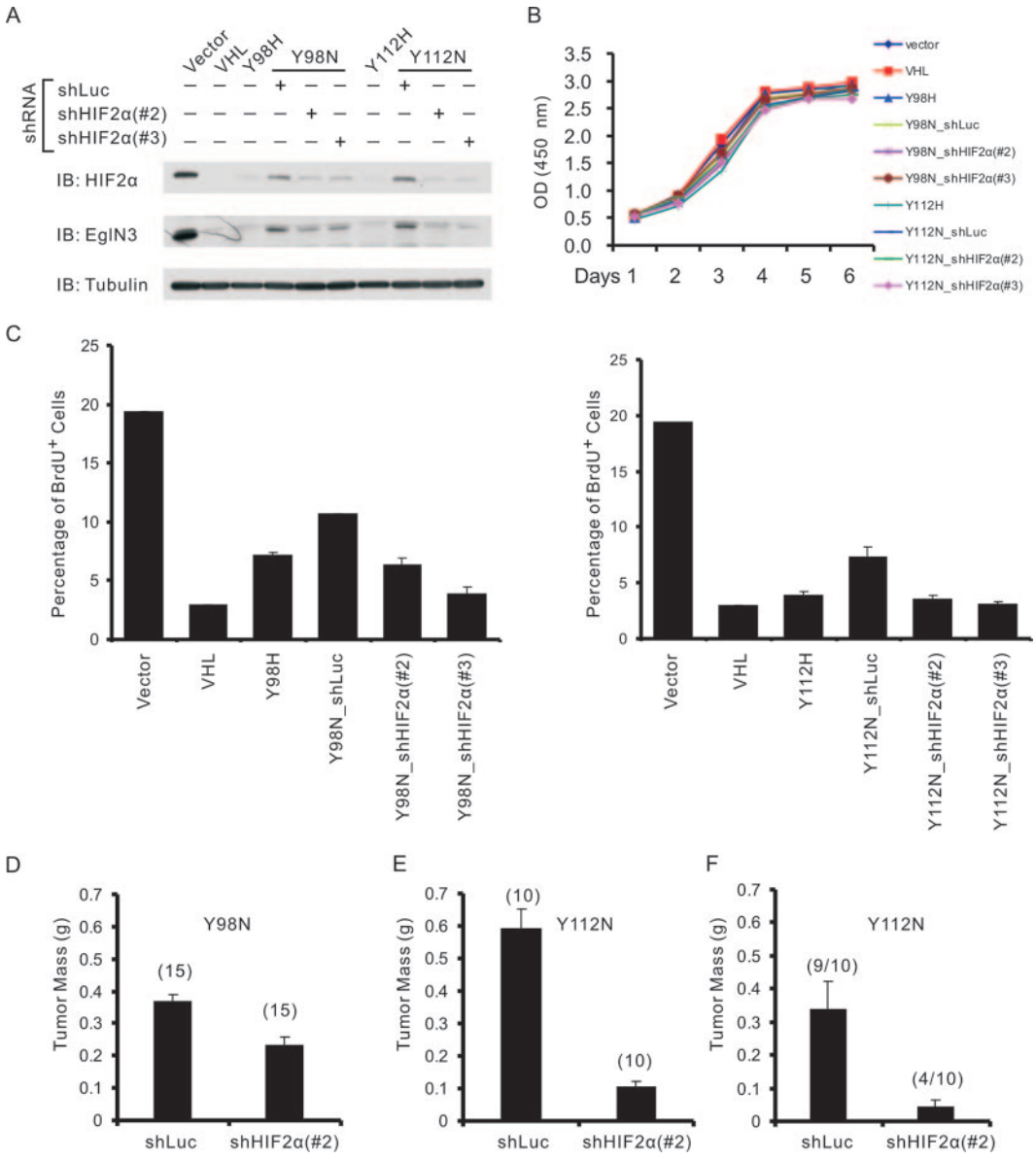

FIG. 6. HIF2α downregulation in 786-O cells producing type 2B mutants results in decreased tumorigenicity in vivo. (A) Immunoblot (IB) analysis of 786-O cells producing the indicated pVHL variants (or infected with empty vector) and subsequently infected with retroviruses encoding shRNAs targeting HIF2α [shHIF2α(#2) and shHIF2α(#3)] or luciferase (shLuc). (B) Optical density (OD) at 450 nm, which reflects viable cell number, of 786-O cells studied in panel A and maintained in 10% fetal bovine serum. Standard deviation is <0.2 for all data points. (C) BrdU incorporation of 786-O cells stably infected with retroviruses as in panel A and maintained in serum-free DMEM supplemented with 1% insulin-transferrin-selenium (1% ITS) for 72 h prior to BrdU pulse for 2 h. Error bars indicate standard deviations. (D and E) Masses of tumors formed by 786-O cells stably infected with retroviruses as in panel A 8 weeks after subcutaneous injection in nude mice. Each mouse was injected with cells expressing luciferase shRNA or HIF2α shRNA on opposite flanks. The number of tumors analyzed is indicated in parentheses. Error bars indicate 1 standard error of the mean ($P < 0.05$). (F) Calculated masses of tumors formed by 786-O cells stably infected with a retrovirus encoding pVHL(Y112N) and the indicated shRNA retrovirus 10 weeks after intraparenchymal renal injection in nude mice. The presence of tumor cells was confirmed by hematoxylin and eosin staining. The tumor mass was calculated by subtracting the mass of the left kidney (normal) from the mass of the right kidney (implanted with tumor). Numbers in parentheses indicate the number of animals with tumors divided by the number of animals injected. Error bars indicate 1 standard error of the mean ($P < 0.05$).

drawal (Fig. 6C), such that the type 2B cells now behaved similarly to the cells producing the corresponding type 2A mutants, and downregulation of HIF2α suppressed tumor formation in vivo when cells were planted subcutaneously in the flanks of nude mice (Fig. 6D and E). Likewise, downregulation of HIF2α in Y112N cells diminished tumor growth in orthotopic assays (Fig. 6F). Therefore, differences in HIF regulation cause, and do not merely correlate with, the observed differences between cells producing type 2A and type 2B pVHL mutants with respect to tumor formation in vivo.

DISCUSSION

Genotype-phenotype correlations have emerged with respect to the organ-specific risk of tumor development in VHL disease. In the present study we focused on potential explanations for the different phenotypes that define type 2A and type 2B VHL disease. Type 2A disease is characterized by a low risk of renal carcinoma, and type 2B disease is characterized by a high risk of renal carcinoma. We found that type 2A mutants are less defective than type 2B pVHL mutants with respect to downregulation of the canonical pVHL target HIFα when reintroduced into $VHL^{-/-}$ cells, in keeping with the recent report that type 2A mutants bind to HIFα with higher affinity than type 2B mutants in vitro (46). $VHL^{-/-}$ renal carcinoma cells engineered to produce type 2B mutants produced larger tumors than cells producing type 2A mutants. Downregulation of HIF2α in the former reduced tumor growth while a stabilized version of HIF2α promoted tumor growth by the latter. Gene expression profiling confirmed quantitative differences between type 2A mutants and type 2B mutants related to the regulation of HIF target genes and did not reveal substantial qualitative differences. Collectively, these results suggest that quantitative differences with respect to HIF deregulation are the basis of the differential risk of renal carcinoma linked to type 2A and type 2B mutants. While type 2A and type 2B mutants might also differ with respect to HIF-independent functions, one need not invoke such differences to explain their different risks of renal carcinoma in humans.

Over 50% of sporadic clear cell renal carcinomas are characterized by pVHL inactivation (43). The present study adds to the mounting evidence implicating deregulation of HIF in the development of pVHL-defective renal carcinoma. Stabilized versions of HIF2α, such as the one used here, can prevent pVHL from suppressing the growth of $VHL^{-/-}$ renal carcinoma cells in vivo, as can peptides that bind to the pVHL HIF-binding domain (47, 48, 55). Conversely, elimination of HIF2α using shRNA technology is sufficient to suppress $VHL^{-/-}$ tumor growth (47, 79). HIF activates a number of genes implicated in renal carcinogenesis including *VEGF*, *PDGF*, and *TGFA* (38). In addition, increased HIF indirectly downregulates molecules such as E-cadherin, thereby promoting an epithelial to mesenchymal transition (18, 19, 49). Notably, agents that indirectly downregulate HIF, such as the mammalian target of rapamycin inhibitor CCI-779, or that interfere with signaling by VEGF and PDGF, such as the drugs sorafenib and sunitinib, have been proven to delay tumor progression in phase III kidney cancer trials (8, 28).

A critical role for HIF in pVHL-defective tumor development is also supported by mouse models. $VHL^{+/-}$ mice, in contrast to their human counterparts, spontaneously develop liver pathology and not kidney cancer (23, 53). In a recent study, expressing stabilized versions of HIF1α and HIF2α in mouse liver induced changes that were indistinguishable from those observed following conditional inactivation of *VHL* (44). At the same time, elimination of the HIFα heterodimeric partner HIF1β prevented the development of pathology after *VHL* inactivation in the mouse liver (67).

Given the above, why do patients with type 2A mutations, like those with type 2B mutations, display an increased risk of both hemangioblastoma and pheochromocytoma? In the case of hemangioblastoma, deregulation of HIF almost certainly plays a contributory role in tumorigenesis (36, 43). These are highly vascular tumors that characteristically overproduce VEGF, and deregulated VEGF expression in mouse models cause the development of hemangioblastoma-like lesions (4). We hypothesize that lower levels of HIF are required to promote hemangioblastoma development than are required to promote renal tumorigenesis. In this model, HIF levels associated with type 2A mutants exceed the threshold required for hemangioblastoma development but not the threshold required for kidney cancer development. It should be noted that cells producing type 2A pVHL mutants at physiological levels would probably display even higher levels of HIF than documented here since overproducing these mutants would potentially compensate for their decreased binding affinity for HIF.

TABLE 1. Characteristics of different types of VHL disease

Type of VHL disease	*VHL* mutation type	Tumor type			Relative amt of HIF
		HB	RCC	Pheo	
1	Deletion, nonsense, missense	+	+	−	↑ ↑ ↑
2B	Missense	+	+	+	↑ ↑
2A	Missense	+	−	+	↑
2C	Missense	−	−	+	~Normal

[a] HB, hemangioblastomas; Pheo, pheochromocytoma.

Pheochromocytomas (intra-adrenal paragangliomas) and extra-adrenal paragangliomas are derived from the same precursors that give rise to the sympathetic nervous system and also display increased levels of HIF (11, 66, 73). However, some VHL families present as familial pheochromocytoma without the other stigmata of VHL disease (type 2C disease). When tested, the *VHL* alleles linked to type 2C disease, such as L188V, are seemingly wild type with respect to HIF deregulation (7, 26). This suggests that even very subtle HIF defects are sufficient to promote pheochromocytoma or that pheochromocytoma development is a manifestation of a HIF-independent pVHL function. In this regard, we recently showed that type 2C pVHL mutants are defective with respect to HIF-independent regulation of atypical protein kinase C and JunB, which is capable of blocking neuronal apoptosis when growth factors such as nerve growth factor become limiting (50). Moreover, this process would predictably be altered by the other genes linked to familial paraganglioma syndromes (50). In addition, we found that the HIF-responsive gene product EglN3 promotes neuronal apoptosis, perhaps accounting for the low risk of pheochromocytoma in patients with null *VHL* alleles (type 1) (50).

Based on these findings and previous work, we suggest that quantitative differences with respect to HIF regulation are the major determinant of the genotype-phenotype correlations in VHL disease. Mutations that measurably deregulate HIF cause hemangioblastoma (as seen in type 1, 2A, and 2B disease) (Table 1). A higher amount of HIF is required for renal carcinoma (as seen in type 1 and 2B disease) than for hemangioblastoma. Pheochromocytoma (a feature of type 2 disease) is largely caused by deregulation of atypical protein kinase C and JunB, perhaps with a modest contributory role for HIF in the case of type 2A and type 2B mutations. However, exceed-

ingly high levels of HIF, such as occur with null *VHL* alleles, would prevent pheochromocytoma development (type 1). This would explain why over 90% of *VHL* mutations linked to pheochromocytoma are missense mutations, whereas gross deletions and truncations are linked to type 1 disease (6, 9).

ACKNOWLEDGMENTS

We thank members of the Kaelin laboratory for critical reading of the manuscript and for useful discussion. We also thank Sabina Signoretti and the Dana-Farber/Harvard Cancer Center Specialized Histopathology Core for excellent help with histopathology studies.

This work was supported by grants from the NIH (to W.G.K.), Murray Foundation (to W.G.K.), and by a career development award from the Dana-Farber/Harvard Renal SPORE (to L.L.). W.G.K. is an HHMI Investigator. Rosetta Inpharmatics LLC is a wholly owned subsidiary of Merck & Co.

REFERENCES

1. **An, Z., P. Jiang, X. Wang, A. R. Moossa, and R. M. Hoffman.** 1999. Development of a high metastatic orthotopic model of human renal cell carcinoma in nude mice: benefits of fragment implantation compared to cell-suspension injection. Clin. Exp. Metastasis **17:**265–270.
2. **Appelhoff, R. J., Y. M. Tian, R. R. Raval, H. Turley, A. L. Harris, C. W. Pugh, P. J. Ratcliffe, and J. M. Gleadle.** 2004. Differential function of the prolyl hydroxylases PHD1, PHD2, and PHD3 in the regulation of hypoxia-inducible factor. J. Biol. Chem. **279:**38458–38465.
3. **Aprelikova, O., G. V. Chandramouli, M. Wood, J. R. Vasselli, J. Riss, J. K. Maranchie, W. M. Linehan, and J. C. Barrett.** 2004. Regulation of HIF prolyl hydroxylases by hypoxia-inducible factors. J. Cell Biochem. **92:**491–501.
4. **Benjamin, L. E., and E. Keshet.** 1997. Conditional switching of vascular endothelial growth factor (VEGF) expression in tumors: induction of endothelial cell shedding and regression of hemangioblastoma-like vessels by VEGF withdrawal. Proc. Natl. Acad. Sci. USA **94:**8761–8766.
5. **Bruick, R. K., and S. L. McKnight.** 2001. A conserved family of prolyl-4-hydroxylases that modify HIF. Science **294:**1337–1340.
6. **Chen, F., T. Kishida, M. Yao, T. Hustad, D. Glavac, M. Dean, J. R. Gnarra, M. L. Orcutt, F. M. Duh, G. Glenn, et al.** 1995. Germline mutations in the von Hippel-Lindau disease tumor suppressor gene: correlations with phenotype. Hum. Mutat. **5:**66–75.
7. **Clifford, S. C., M. E. Cockman, A. C. Smallwood, D. R. Mole, E. R. Woodward, P. H. Maxwell, P. J. Ratcliffe, and E. R. Maher.** 2001. Contrasting effects on HIF-1alpha regulation by disease-causing pVHL mutations correlate with patterns of tumourigenesis in von Hippel-Lindau disease. Hum. Mol. Genet. **10:**1029–1038.
8. **Cohen, H. T., and F. J. McGovern.** 2005. Renal-cell carcinoma. N. Engl. J. Med. **353:**2477–2490.
9. **Crossey, P. A., F. M. Richards, K. Foster, J. S. Green, A. Prowse, F. Latif, M. I. Lerman, B. Zbar, N. A. Affara, M. A. Ferguson-Smith, et al.** 1994. Identification of intragenic mutations in the von Hippel-Lindau disease tumour suppressor gene and correlation with disease phenotype. Hum. Mol. Genet. **3:**1303–1308.
10. **Czyzyk-Krzeska, M. F., and J. Meller.** 2004. von Hippel-Lindau tumor suppressor: not only HIF's executioner. Trends Mol. Med. **10:**146–149.
11. **Dahia, P. L., K. N. Ross, M. E. Wright, C. Y. Hayashida, S. Santagata, M. Barontini, A. L. Kung, G. Sanso, J. F. Powers, A. S. Tischler, R. Hodin, S. Heitritter, F. Moore, R. Dluhy, J. A. Sosa, I. T. Ocal, D. E. Benn, D. J. Marsh, B. G. Robinson, K. Schneider, J. Garber, S. M. Arum, M. Korbonits, A. Grossman, P. Pigny, S. P. Toledo, V. Nose, C. Li, and C. D. Stiles.** 2005. A HIF1α regulatory loop links hypoxia and mitochondrial signals in pheochromocytomas. PLOS Genet. **1:**72–80.
12. **Davidowitz, E. J., A. R. Schoenfeld, and R. D. Burk.** 2001. VHL induces renal cell differentiation and growth arrest through integration of cell-cell and cell-extracellular matrix signaling. Mol. Cell. Biol. **21:**865–874.
13. **del Peso, L., M. C. Castellanos, E. Temes, S. Martin-Puig, Y. Cuevas, G. Olmos, and M. O. Landazuri.** 2003. The von Hippel Lindau/hypoxia-inducible factor (HIF) pathway regulates the transcription of the HIF-proline hydroxylase genes in response to low oxygen. J. Biol. Chem. **278:**48690–48695.
14. **de Paulsen, N., A. Brychzy, M. C. Fournier, R. D. Klausner, J. R. Gnarra, A. Pause, and S. Lee.** 2001. Role of transforming growth factor-alpha in von Hippel-Lindau (VHL) (−/−) clear cell renal carcinoma cell proliferation: a possible mechanism coupling VHL tumor suppressor inactivation and tumorigenesis. Proc. Natl. Acad. Sci. USA **98:**1387–1392.
15. **Duan, D. R., J. S. Humphrey, D. Y. Chen, Y. Weng, J. Sukegawa, S. Lee, J. R. Gnarra, W. M. Linehan, and R. D. Klausner.** 1995. Characterization of the VHL tumor suppressor gene product: localization, complex formation, and the effect of natural inactivating mutations. Proc. Natl. Acad. Sci. USA **92:**6459–6463.
16. **Duan, D. R., A. Pause, W. H. Burgess, T. Aso, D. Y. Chen, K. P. Garrett, R. C. Conaway, J. W. Conaway, W. M. Linehan, and R. D. Klausner.** 1995. Inhibition of transcription elongation by the VHL tumor suppressor protein. Science **269:**1402–1406.
17. **Epstein, A. C., J. M. Gleadle, L. A. McNeill, K. S. Hewitson, J. O'Rourke, D. R. Mole, M. Mukherji, E. Metzen, M. I. Wilson, A. Dhanda, Y. M. Tian, N. Masson, D. L. Hamilton, P. Jaakkola, R. Barstead, J. Hodgkin, P. H. Maxwell, C. W. Pugh, C. J. Schofield, and P. J. Ratcliffe.** 2001. *C. elegans* EGL-9 and mammalian homologs define a family of dioxygenases that regulate HIF by prolyl hydroxylation. Cell **107:**43–54.
18. **Esteban, M. A., M. G. Tran, S. K. Harten, P. Hill, M. C. Castellanos, A. Chandra, R. Raval, T. S. O'Brien, and P. H. Maxwell.** 2006. Regulation of E-cadherin expression by VHL and hypoxia-inducible factor. Cancer Res. **66:**3567–3575.
19. **Evans, A. J., R. C. Russell, O. Roche, T. N. Burry, J. E. Fish, V. W. Chow, W. Y. Kim, A. Saravanan, M. A. Maynard, M. L. Gervais, R. I. Sufan, A. M. Roberts, L. A. Wilson, M. Betten, C. Vandewalle, G. Berx, P. A. Marsden, M. S. Irwin, B. T. Teh, M. A. Jewett, and M. Ohh.** 2007. VHL Promotes E2 box-dependent E-cadherin transcription by HIF-mediated regulation of SIP1 and Snail. Mol. Cell. Biol. **27:**157–169.
20. **Fidler, I. J., S. Naito, and S. Pathak.** 1990. Orthotopic implantation is essential for the selection, growth and metastasis of human renal cell cancer in nude mice. Cancer Metastasis Rev. **9:**149–165. (Erratum, **10:**79, 1991.)
21. **Gnarra, J. R., S. Zhou, M. J. Merrill, J. R. Wagner, A. Krumm, E. Papavassiliou, E. H. Oldfield, R. D. Klausner, and W. M. Linehan.** 1996. Post-transcriptional regulation of vascular endothelial growth factor mRNA by the product of the VHL tumor suppressor gene. Proc. Natl. Acad. Sci. USA **93:**10589–10594.
22. **Gunaratnam, L., M. Morley, A. Franovic, N. de Paulsen, K. Mekhail, D. A. Parolin, E. Nakamura, I. A. Lorimer, and S. Lee.** 2003. Hypoxia inducible factor activates the transforming growth factor-alpha/epidermal growth factor receptor growth stimulatory pathway in VHL(−/−) renal cell carcinoma cells. J. Biol. Chem. **278:**44966–44974.
23. **Haase, V. H., J. N. Glickman, M. Socolovsky, and R. Jaenisch.** 2001. Vascular tumors in livers with targeted inactivation of the von Hippel-Lindau tumor suppressor. Proc. Natl. Acad. Sci. USA **98:**1583–1588.
24. **Harris, A. L.** 2002. Hypoxia—a key regulatory factor in tumour growth. Nat. Rev. Cancer **2:**38–47.
25. **Hergovich, A., J. Lisztwan, R. Barry, P. Ballschmieter, and W. Krek.** 2003. Regulation of microtubule stability by the von Hippel-Lindau tumour suppressor protein pVHL. Nat. Cell Biol. **5:**64–70.
26. **Hoffman, M. A., M. Ohh, H. Yang, J. M. Klco, M. Ivan, and W. G. Kaelin, Jr.** 2001. von Hippel-Lindau protein mutants linked to type 2C VHL disease preserve the ability to downregulate HIF. Hum. Mol. Genet. **10:**1019–1027.
27. **Hon, W. C., M. I. Wilson, K. Harlos, T. D. Claridge, C. J. Schofield, C. W. Pugh, P. H. Maxwell, P. J. Ratcliffe, D. I. Stuart, and E. Y. Jones.** 2002. Structural basis for the recognition of hydroxyproline in HIF-1 alpha by pVHL. Nature **417:**975–978.
28. **Hudes, G., M. Carducci, J. Tomczak, J. Dutcher, R. Figlin, A. Kapoor, E. Staroslawska, T. O'Toole, Y. Park, and L. Moore.** 2006. A phase 3, randomized, 3-arm study of temsirolimus (TEMSR) or interferon-alpha (IFN) or the combination of TEMSR + IFN in the treatment of first-line, poor-risk patients with advanced renal cell carcinoma (adv RCC), abstr. LBA4. *In* 2006 ASCO annual meetings proceedings, part I. J. Clin. Oncol. **24:**18S.
29. **Hughes, T. R., M. Mao, A. R. Jones, J. Burchard, M. J. Marton, K. W. Shannon, S. M. Lefkowitz, M. Ziman, J. M. Schelter, M. R. Meyer, S. Kobayashi, C. Davis, H. Dai, Y. D. He, S. B. Stephaniants, G. Cavet, W. L. Walker, A. West, E. Coffey, D. D. Shoemaker, R. Stoughton, A. P. Blanchard, S. H. Friend, and P. S. Linsley.** 2001. Expression profiling using microarrays fabricated by an ink-jet oligonucleotide synthesizer. Nat. Biotechnol. **19:**342–347.
30. **Iliopoulos, O., A. Kibel, S. Gray, and W. G. Kaelin, Jr.** 1995. Tumour suppression by the human von Hippel-Lindau gene product. Nat. Med. **1:**822–826.
31. **Ivan, M., T. Haberberger, D. C. Gervasi, K. S. Michelson, V. Gunzler, K. Kondo, H. Yang, I. Sorokina, R. C. Conaway, J. W. Conaway, and W. G. Kaelin, Jr.** 2002. Biochemical purification and pharmacological inhibition of a mammalian prolyl hydroxylase acting on hypoxia-inducible factor. Proc. Natl. Acad. Sci. USA **99:**13459–13464.
32. **Ivan, M., K. Kondo, H. Yang, W. Kim, J. Valiando, M. Ohh, A. Salic, J. M. Asara, W. S. Lane, and W. G. Kaelin, Jr.** 2001. HIFα targeted for VHL-mediated destruction by proline hydroxylation: implications for O2 sensing. Science **292:**464–468.
33. **Iwai, K., K. Yamanaka, T. Kamura, N. Minato, R. C. Conaway, J. W. Conaway, R. D. Klausner, and A. Pause.** 1999. Identification of the von Hippel-Lindau tumor-suppressor protein as part of an active E3 ubiquitin ligase complex. Proc. Natl. Acad. Sci. USA **96:**12436–12441.
34. **Jaakkola, P., D. R. Mole, Y. M. Tian, M. I. Wilson, J. Gielbert, S. J. Gaskell, A. Kriegsheim, H. F. Hebestreit, M. Mukherji, C. J. Schofield, P. H. Maxwell, C. W. Pugh, and P. J. Ratcliffe.** 2001. Targeting of HIF-alpha to the

von Hippel-Lindau ubiquitylation complex by O2-regulated prolyl hydroxylation. Science **292:**468–472.
35. **Kaelin, W. G.** 2005. Proline hydroxylation and gene expression. Annu. Rev. Biochem. **74:**115–128.
36. **Kaelin, W. G., Jr.** 2002. Molecular basis of the VHL hereditary cancer syndrome. Nat. Rev. Cancer **2:**673–682.
37. **Kaelin, W. G., Jr.** 2005. The von Hippel-Lindau protein, HIF hydroxylation, and oxygen sensing. Biochem. Biophys. Res. Commun. **338:**627–638.
38. **Kaelin, W. G., Jr.** 2004. The von Hippel-Lindau tumor suppressor gene and kidney cancer. Clin. Cancer Res. **10:**6290S–6295S.
39. **Kamura, T., M. N. Conrad, Q. Yan, R. C. Conaway, and J. W. Conaway.** 1999. The Rbx1 subunit of SCF and VHL E3 ubiquitin ligase activates Rub1 modification of cullins Cdc53 and Cul2. Genes Dev. **13:**2928–2933.
40. **Kamura, T., D. M. Koepp, M. N. Conrad, D. Skowyra, R. J. Moreland, O. Iliopoulos, W. S. Lane, W. G. Kaelin, Jr., S. J. Elledge, R. C. Conaway, J. W. Harper, and J. W. Conaway.** 1999. Rbx1, a component of the VHL tumor suppressor complex and SCF ubiquitin ligase. Science **284:**657–661.
41. **Kamura, T., K. Maenaka, S. Kotoshiba, M. Matsumoto, D. Kohda, R. C. Conaway, J. W. Conaway, and K. I. Nakayama.** 2004. VHL-box and SOCS-box domains determine binding specificity for Cul2-Rbx1 and Cul5-Rbx2 modules of ubiquitin ligases. Genes Dev. **18:**3055–3065.
42. **Kibel, A., O. Iliopoulos, J. A. DeCaprio, and W. G. Kaelin, Jr.** 1995. Binding of the von Hippel-Lindau tumor suppressor protein to elongin B and C. Science **269:**1444–1446.
43. **Kim, W. Y., and W. G. Kaelin.** 2004. Role of VHL gene mutation in human cancer. J. Clin. Oncol. **22:**4991–5004.
44. **Kim, W. Y., M. Safran, M. R. Buckley, B. L. Ebert, J. Glickman, M. Bosenberg, M. Regan, and W. G. Kaelin, Jr.** 2006. Failure to prolyl hydroxylate hypoxia-inducible factor alpha phenocopies VHL inactivation in vivo. EMBO J. **25:**4650–4662.
45. **Kishida, T., T. M. Stackhouse, F. Chen, M. I. Lerman, and B. Zbar.** 1995. Cellular proteins that bind the von Hippel-Lindau disease gene product: mapping of binding domains and the effect of missense mutations. Cancer Res. **55:**4544–4548.
46. **Knauth, K., C. Bex, P. Jemth, and A. Buchberger.** 2006. Renal cell carcinoma risk in type 2 von Hippel-Lindau disease correlates with defects in pVHL stability and HIF-1α interactions. Oncogene **25:**370–377.
47. **Kondo, K., W. Y. Kim, M. Lechpammer, and W. G. Kaelin, Jr.** 2003. Inhibition of HIF2α is sufficient to suppress pVHL-defective tumor growth. PLOS Biol. **1:**E83.
48. **Kondo, K., J. Klco, E. Nakamura, M. Lechpammer, and W. G. Kaelin, Jr.** 2002. Inhibition of HIF is necessary for tumor suppression by the von Hippel-Lindau protein. Cancer Cell **1:**237–246.
49. **Krishnamachary, B., D. Zagzag, H. Nagasawa, K. Rainey, H. Okuyama, J. H. Baek, and G. L. Semenza.** 2006. Hypoxia-inducible factor-1-dependent repression of E-cadherin in von Hippel-Lindau tumor suppressor-null renal cell carcinoma mediated by TCF3, ZFHX1A, and ZFHX1B. Cancer Res. **66:**2725–2731.
50. **Lee, S., E. Nakamura, H. Yang, W. Wei, M. S. Linggi, M. P. Sajan, R. V. Farese, R. S. Freeman, B. D. Carter, W. G. Kaelin, Jr., and S. Schlisio.** 2005. Neuronal apoptosis linked to EglN3 prolyl hydroxylase and familial pheochromocytoma genes: developmental culling and cancer. Cancer Cell **8:**155–167.
51. **Lieubeau-Teillet, B., J. Rak, S. Jothy, O. Iliopoulos, W. Kaelin, and R. S. Kerbel.** 1998. von Hippel-Lindau gene-mediated growth suppression and induction of differentiation in renal cell carcinoma cells grown as multicellular tumor spheroids. Cancer Res. **58:**4957–4962.
52. **Lonergan, K. M., O. Iliopoulos, M. Ohh, T. Kamura, R. C. Conaway, J. W. Conaway, and W. G. Kaelin, Jr.** 1998. Regulation of hypoxia-inducible mRNAs by the von Hippel-Lindau tumor suppressor protein requires binding to complexes containing elongins B/C and Cul2. Mol. Cell. Biol. **18:**732–741.
53. **Ma, W., L. Tessarollo, S. B. Hong, M. Baba, E. Southon, T. C. Back, S. Spence, C. G. Lobe, N. Sharma, G. W. Maher, S. Pack, A. O. Vortmeyer, C. Guo, B. Zbar, and L. S. Schmidt.** 2003. Hepatic vascular tumors, angiectasis in multiple organs, and impaired spermatogenesis in mice with conditional inactivation of the VHL gene. Cancer Res. **63:**5320–5328.
54. **Mandriota, S. J., K. J. Turner, D. R. Davies, P. G. Murray, N. V. Morgan, H. M. Sowter, C. C. Wykoff, E. R. Maher, A. L. Harris, P. J. Ratcliffe, and P. H. Maxwell.** 2002. HIF activation identifies early lesions in VHL kidneys: evidence for site-specific tumor suppressor function in the nephron. Cancer Cell **1:**459–468.
55. **Maranchie, J. K., J. R. Vasselli, J. Riss, J. S. Bonifacino, W. M. Linehan, and R. D. Klausner.** 2002. The contribution of VHL substrate binding and HIF1-α to the phenotype of VHL loss in renal cell carcinoma. Cancer Cell **1:**247–255.
56. **Masson, N., C. Willam, P. H. Maxwell, C. W. Pugh, and P. J. Ratcliffe.** 2001. Independent function of two destruction domains in hypoxia-inducible factor-alpha chains activated by prolyl hydroxylation. EMBO J. **20:**5197–5206.
57. **Maxwell, P. H., M. S. Wiesener, G. W. Chang, S. C. Clifford, E. C. Vaux, M. E. Cockman, C. C. Wykoff, C. W. Pugh, E. R. Maher, and P. J. Ratcliffe.** 1999. The tumour suppressor protein VHL targets hypoxia-inducible factors for oxygen-dependent proteolysis. Nature **399:**271–275.
58. **Min, J. H., H. Yang, M. Ivan, F. Gertler, W. G. Kaelin, Jr., and N. P. Pavletich.** 2002. Structure of an HIF-1α-pVHL complex: hydroxyproline recognition in signaling. Science **296:**1886–1889.
59. **Naito, S., S. M. Walker, and I. J. Fidler.** 1989. In vivo selection of human renal cell carcinoma cells with high metastatic potential in nude mice. Clin. Exp. Metastasis **7:**381–389.
60. **Nakamura, E., P. Abreu-e-Lima, Y. Awakura, T. Inoue, T. Kamoto, O. Ogawa, H. Kotani, T. Manabe, G. J. Zhang, K. Kondo, V. Nose, and W. G. Kaelin, Jr.** 2006. Clusterin is a secreted marker for a hypoxia-inducible factor-independent function of the von Hippel-Lindau tumor suppressor protein. Am. J. Pathol **168:**574–584.
61. **Ohh, M., C. W. Park, M. Ivan, M. A. Hoffman, T. Y. Kim, L. E. Huang, N. Pavletich, V. Chau, and W. G. Kaelin.** 2000. Ubiquitination of hypoxia-inducible factor requires direct binding to the beta-domain of the von Hippel-Lindau protein. Nat. Cell Biol. **2:**423–427.
62. **Ohh, M., Y. Takagi, T. Aso, C. E. Stebbins, N. P. Pavletich, B. Zbar, R. C. Conaway, J. W. Conaway, and W. G. Kaelin, Jr.** 1999. Synthetic peptides define critical contacts between elongin C, elongin B, and the von Hippel-Lindau protein. J. Clin. Investig. **104:**1583–1591.
63. **Pause, A., S. Lee, K. M. Lonergan, and R. D. Klausner.** 1998. The von Hippel-Lindau tumor suppressor gene is required for cell cycle exit upon serum withdrawal. Proc. Natl. Acad. Sci. USA **95:**993–998.
64. **Pause, A., S. Lee, R. A. Worrell, D. Y. Chen, W. H. Burgess, W. M. Linehan, and R. D. Klausner.** 1997. The von Hippel-Lindau tumor-suppressor gene product forms a stable complex with human CUL-2, a member of the Cdc53 family of proteins. Proc. Natl. Acad. Sci. USA **94:**2156–2161.
65. **Pescador, N., Y. Cuevas, S. Naranjo, M. Alcaide, D. Villar, M. O. Landazuri, and L. Del Peso.** 2005. Identification of a functional hypoxia-responsive element that regulates the expression of the *egl nine* homologue 3 (*egln3*/*phd3*) gene. Biochem. J. **390:**189–197.
66. **Pollard, P. J., J. J. Briere, N. A. Alam, J. Barwell, E. Barclay, N. C. Wortham, T. Hunt, M. Mitchell, S. Olpin, S. J. Moat, I. P. Hargreaves, S. J. Heales, Y. L. Chung, J. R. Griffiths, A. Dalgleish, J. A. McGrath, M. J. Gleeson, S. V. Hodgson, R. Poulsom, P. Rustin, and I. P. Tomlinson.** 2005. Accumulation of Krebs cycle intermediates and over-expression of HIF1α in tumours which result from germline FH and SDH mutations. Hum. Mol. Genet. **14:**2231–2239.
67. **Rankin, E. B., D. F. Higgins, J. A. Walisser, R. S. Johnson, C. A. Bradfield, and V. H. Haase.** 2005. Inactivation of the arylhydrocarbon receptor nuclear translocator (Arnt) suppresses von Hippel-Lindau disease-associated vascular tumors in mice. Mol. Cell. Biol. **25:**3163–3172.
68. **Rathmell, W. K., M. M. Hickey, N. A. Bezman, C. A. Chmielecki, N. C. Carraway, and M. C. Simon.** 2004. In vitro and in vivo models analyzing von Hippel-Lindau disease-specific mutations. Cancer Res. **64:**8595–8603.
69. **Raval, R. R., K. W. Lau, M. G. Tran, H. M. Sowter, S. J. Mandriota, J. L. Li, C. W. Pugh, P. H. Maxwell, A. L. Harris, and P. J. Ratcliffe.** 2005. Contrasting properties of hypoxia-inducible factor 1 (HIF-1) and HIF-2 in von Hippel-Lindau-associated renal cell carcinoma. Mol. Cell. Biol. **25:**5675–5686.
70. **Richard, S., R. Lidereau, and S. Giraud.** 2004. The growing family of hereditary renal cell carcinoma. Nephrol. Dial. Transplant. **19:**2954–2958.
71. **Schoenfeld, A. R., E. J. Davidowitz, and R. D. Burk.** 2000. Elongin BC complex prevents degradation of von Hippel-Lindau tumor suppressor gene products. Proc. Natl. Acad. Sci. USA **97:**8507–8512.
72. **Schofield, C. J., and P. J. Ratcliffe.** 2004. Oxygen sensing by HIF hydroxylases. Nat. Rev. Mol. Cell. Biol. **5:**343–354.
73. **Selak, M. A., S. M. Armour, E. D. MacKenzie, H. Boulahbel, D. G. Watson, K. D. Mansfield, Y. Pan, M. C. Simon, C. B. Thompson, and E. Gottlieb.** 2005. Succinate links TCA cycle dysfunction to oncogenesis by inhibiting HIF-α prolyl hydroxylase. Cancer Cell **7:**77–85.
74. **Smith, K., L. Gunaratnam, M. Morley, A. Franovic, K. Mekhail, and S. Lee.** 2005. Silencing of epidermal growth factor receptor suppresses hypoxia-inducible factor-2-driven VHL$^{-/-}$ renal cancer. Cancer Res. **65:**5221–5230.
75. **Staller, P., J. Sulitkova, J. Lisztwan, H. Moch, E. J. Oakeley, and W. Krek.** 2003. Chemokine receptor CXCR4 downregulated by von Hippel-Lindau tumour suppressor pVHL. Nature **425:**307–311.
76. **Stebbins, C. E., W. G. Kaelin, Jr., and N. P. Pavletich.** 1999. Structure of the VHL-elongin C-elongin B complex: implications for VHL tumor suppressor function. Science **284:**455–461.
77. **Yu, F., S. B. White, Q. Zhao, and F. S. Lee.** 2001. HIF-1α binding to VHL is regulated by stimulus-sensitive proline hydroxylation. Proc. Natl. Acad. Sci. USA **98:**9630–9635.
78. **Zagzag, D., B. Krishnamachary, H. Yee, H. Okuyama, L. Chiriboga, M. A. Ali, J. Melamed, and G. L. Semenza.** 2005. Stromal cell-derived factor-1α and CXCR4 expression in hemangioblastoma and clear cell-renal cell carcinoma: von Hippel-Lindau loss-of-function induces expression of a ligand and its receptor. Cancer Res. **65:**6178–6188.
79. **Zimmer, M., D. Doucette, N. Siddiqui, and O. Iliopoulos.** 2004. Inhibition of hypoxia-inducible factor is sufficient for growth suppression of VHL$^{-/-}$ tumors. Mol. Cancer Res. **2:**89–95.